ANTIOXIDANTS & REDOX SIGNALING
Volume 14, Number 11, 2011

DOI: 10.1089/ars.2010.3263

ORIGINAL RESEARCH COMMUNICATION

Role of the Inducible Nitric Oxide Synthase in the Onset of Fructose-Induced Steatosis in Mice

Astrid Spruss, Giridhar Kanuri, Kirsten Uebel, Stephan C. Bischoff, and Ina Bergheim

Abstract

To test the hypothesis that the inducible nitric oxide synthase (iNOS) is involved in mediating the toll-like receptor 4-dependent effects on the liver in the onset of fructose-induced steatosis, wild-type and iNOS knockout ($iNOS^{-/-}$) mice were either fed tap water or 30% fructose solution for 8 weeks. Chronic consumption of 30% fructose solution led to a significant increase in hepatic steatosis and inflammation as well as plasma alanine-aminotransferase levels in wild-type mice. This effect of fructose feeding was markedly attenuated in $iNOS^{-/-}$ mice. Hepatic lipidperoxidation, concentration of phospho-IκB, nuclear factor κB activity, and tumor necrosis factor-α mRNA level were significantly increased in fructose-fed wild-type mice, whereas in livers of fructose-fed $iNOS^{-/-}$ mice, lipidperoxidation, phospho-IκB, nuclear factor κB activity, and tumor necrosis factor-α expression were almost at the level of controls. However, portal endotoxin levels and hepatic myeloid differentiation factor 88 expression were significantly higher in both fructose-fed groups compared to controls. Taken together, these data suggest that (i) the formation of reactive oxygen species in liver is a key factor in the onset of fatty liver and (ii) iNOS is involved in mediating the endotoxin/toll-like receptor 4-dependent effects in the development of fructose-induced fatty liver. *Antioxid. Redox Signal.* 14, 2121–2135.

Introduction

Nonalcoholic fatty liver disease (NAFLD) usually develops in the setting of obesity and insulin resistance and includes a continuum of disease ranging from steatosis to steatohepatitis and cirrhosis (8). During the last years it has become more obvious that steatosis, long been thought to be a relatively benign state of liver injury, is a state of liver disease in which the liver is more vulnerable to injury from various causes (44). Further, steatosis can progress to steatohepatitis, increasing the probability of further liver-related morbidity and mortality (4). As mechanisms involved in the development of NAFLD are not yet fully understood, therapeutic and preventive options are still limited. Therefore, a better understanding of the biochemical and pathological changes that cause the early stages of NAFLD (*e.g.*, steatosis) is desirable to improve prevention but also intervention strategies.

Besides a general overnutrition, a diet rich in carbohydrates and herein particularly in fructose has been discussed to be critically involved in the development of NAFLD. Indeed, results of several human studies suggest that patients with NAFLD (*e.g.*, with simple steatosis and steatohepatitis with beginning fibrosis) consume markedly more fructose in their diet than controls (1, 28, 38). Further, it has been suggested by the results of Solga *et al.* (35) that a high intake of carbohydrates can increase the odds of developing later, more severe stages of the disease (*e.g.*, nonalcoholic steatohepatitis [NASH]). In line with these human findings it has been shown in several animal studies that an increased consumption of fructose (*e.g.*, as chow or drinking solution) may result in hepatic steatosis accompanied by insulin resistance, elevated plasma triglyceride levels, and oxidative stress in the liver (2, 5, 9, 19). Our own group showed recently that already the onset of fructose-induced NAFLD (*e.g.*, steatosis) resulting from an 8-week-long fructose feeding period is associated with an increased translocation of intestinal bacterial endotoxin, formation of 4-hydroxynonenal (4-HNE) adducts, and expression of tumor necrosis factor (TNF)-α in the liver, whereas similar changes were not found in mice fed glucose for 8 weeks (9). Interestingly, in mice concomitantly treated with antibiotics (9) or mice without a functional toll-like receptor 4 (TLR-4), this effect of fructose on the liver was attenuated by $\sim$50% (37). Further, in these mice, the formation of reactive oxygen species (ROS) and the induction of iNOS found in wild-type mice chronically exposed to fructose were markedly reduced.

There is a growing body of evidence implicating that the excessive generation of ROS and herein particularly of nitric oxide (NO) and other reactive nitrogen species is involved

Department of Nutritional Medicine, University of Hohenheim, Stuttgart, Germany.

in the development of various types of liver diseases (*e.g.*, alcoholic liver disease, postischemic liver injury, viral hepatitis, and NASH) (14, 15, 18, 26, 41). Indeed, an induction of iNOS mRNA expression and protein levels as well as increased generation of 3-nitrotyrosine (3-NT) has been demonstrated in a number of different animal models of NASH (*e.g.*, ob/ob, fructose feeding) (25, 34, 37). However, contrary to these reports, Chen *et al.* (12) reported that iNOS may attenuate the progression of steatohepatitis to liver fibrosis in mice fed a high-fat diet. Whether ROS and herein particularly reactive nitrite species and enzymes associated with the formation of ROS are also causally involved in the onset of fructose-induced fatty liver remains to be determined. In the present study we tested the hypothesis that iNOS is (1) involved in the onset of fructose-induced steatosis and (2) mediating, at least in part, the effects of the increased translocation of the endotoxin and subsequent activation of TLR-4-dependent signalling cascades found in chronically fructose-fed animals in a mouse model.

Materials and Methods

Animals and treatments

Eight-week-old C57BL/6J and iNOS$^{-/-}$ mice (B6.129P2-NOS2tm1^{Lau}/J) (Jackson Laboratories, Maine) were housed in a pathogen-free barrier facility in individually ventilated cages, accredited by the Association for Assessment and Accreditation of Laboratory Animal Care (AAALAC). All knockout mice used in this study were backcrossed at least 10 times onto C57BL/6J, avoiding concerns regarding differences between wild-type and knockout mice at nonspecific loci. All procedures were approved by the local Institutional Animal Care and Use Committee (IACUC). For 8 weeks, C57BL/6J and iNOS$^{-/-}$ mice ($n = 4$–6 per group) were either fed plain tap water or water containing 30% fructose *ad libitum*. Throughout the feeding period body weight was assessed weekly. Animals were anesthetized with 80 mg ketamin/kg and 6 mg xylazin/kg body weight by intraperitoneal injection, and blood was collected just before sacrifice. While portions of liver were either frozen immediately in liquid nitrogen, or fixed in neutral-buffered formalin, others were frozen-fixed in OCT mounting media (medite).

Cell culture and treatment

AML-12 cells (alpha mouse liver 12; American Type Culture Collection) were grown in Dulbecco's modified Eagle's medium (DMEM)/F12 (Gibco) supplemented with 10% fetal calf serum, 40 ng/ml dexamethasone, 0.005 mg/ml insulin, and 5 ng/ml selenium (Gibco) in 6-well plates in a humidified 5% CO_2 atmosphere at 37°C until they were 70% confluent. Cells were serum starved for 18 h, and some cells were preincubated with the iNOS inhibitor L-NAME (10 m*M*; Sigma) for 1 h. The medium was subsequently removed and replaced with fresh DMEM/F12 containing fructose (0–50 m*M*) ± L-NAME (25–50 m*M*), and cells were incubated for another 24 h.

Murine RAW 264.7 macrophage-like cells (mouse leukaemic monocyte macrophage cell line; American Type Culture Collection) were grown in DMEM supplemented with 10% fetal calf serum in a humidified 5% CO_2 atmosphere at 37°C. At 70% confluency cells were preincubated with the TLR-4 inhibitor OxPAPC (120 μg/ml; InvivoGen) for 1 h in serum-free media. Then, the cells were stimulated with 50 ng lipopolysaccharide (LPS)/ml in the presence or absence of the TLR-4 inhibitor for 18 h.

After treatment, the medium was taken from both AML-12 as well as RAW 264.7 for later nitrite measurements, and cells were then rinsed with phosphate-buffered saline (PBS), and lysed with peqGOLD TriFast™ (PEQLAB) for later RNA isolation and analysis by real-time reverse transcriptase (RT)–polymerase chain reaction (PCR; see below).

Coculture model and treatment

To investigate the effect of fructose and LPS on Kupffer cells and hepatocytes, a coculture model was developed, in which RAW 264.7 macrophages and AML-12 cells being models of Kupffer cells and murine hepatocytes, respectively, were concomitantly exposed to fructose or LPS in the presence of L-NAME. RAW 264.7 cells were grown on transwell cell culture chambers until ~70% confluence. AML-12 cells were grown in normal six-well plates until ~70% confluence followed by an 18 h serum starvation. Meanwhile, RAW 264.7 cells were challenged with either LPS (50 mg/ml) or fructose (50 m*M*) either in the presence or in the absence of L-NAME (10 m*M*) in DMEM/F12 containing 0.1% bovine serum albumin (BSA) for 1 h. RAW 264.7 cells were then carefully rinsed twice with PBS to wash off excessive LPS or fructose and transwells were placed into the six-well plates, in which AML-12 cells were grown. Fresh starvation medium (DMEM/F12 media [Gibco] supplemented with 0.1% BSA) was added. Some of the cells were additionally treated with L-NAME. After incubation AML-12 as well as RAW cells were harvested separately, rinsed with PBS, and lysed with peqGOLD TriFast™ (PEQLAB) for later RNA isolation and analysis by real-time RT-PCR (see below).

Detection of nitrite

Nitrite levels were deterimend in cell culture media using a commercially available Griess reagent kit (Promega) as detailed before (21).

Clinical chemistry, pathologic evaluation, and ELISAs

Using a commercially available kit (Randox) activity of alanine-aminotransferase (ALT) was determined in plasma of mice. For assessment of liver histology, paraffin-embedded sections of liver (5 μm) were stained with hematoxylin and eosin. Representative photomicrographs were captured at a 400× magnification using a system incorporated in a microscope (Axio Vert 200M) (Zeiss). Further, retinol binding protein (RBP) 4 and TNFα concentration was measured in plasma and concentration of reduced (GSH) as well as oxidized (GSSG) glutathione was determined in liver homogenate of mice using commercially available ELISA kits (GSH and GSSG: Cayman Chemical Company; RBP4: immune diagnostik; TNFα: R&D Systems, respectively). Using a TransAM™ ELISA-based kit (Active Motif) activity of the nuclear factor κB (NFκB) was measured in nuclear extract isolated from liver samples with a lysis buffer (1 *M* HEPES, 50% Glycerol, 5 *M* NaCl, 0.5 *M* EDTA, and 1 *M* DTT) containing a protease and phosphatase inhibitors mix (Sigma) following the instructions of the company.

Hepatic triglyceride determination

Hepatic lipid accumulation was determined as described previously (37) in sections of mouse liver tissue and representative photomicrographs were captured at 400× magnification using a Zeiss microscope (see above). For determination of hepatic triglycerides 2× PBS was used to homogenize frozen liver tissue of mice. After extracting tissue lipids with methanol/chloroform (1:2), lipids were dried and resuspended in 5% fat-free bovine serum albumin. Using a commercially available kit (Randox) triglyceride levels were measured and values were normalized to protein concentration in liver homogenate determined by Bradford assay (Bio Rad Laboratories).

Isolation of RNA and real-time RT-PCR

Using peqGOLD TriFast™ (PEQLAB), total RNA was extracted from liver tissue, and AML-12 and RAW cells, and the concentration of RNA was determined spectrophotometrically. One microgram total RNA was reverse transcribed after a DNase digestion step using MuLV reverse transcriptase and oligo dT primers (Fermentas). PCR primers for myeloid differentiation factor 88 (MyD88) (forward: 5′-CAA AAG TGG GGT GCC TTT GC-3′; reverse: 5′-AAA TCC ACA GTG CCC CCA GA-3′), TNFα (forward: 5′-CCA GGC GGT GCC TAT GTC TC-3′; reverse: 5′-CAG CCA CTC CAG CTG CTC CT-3′), iNOS (forward: 5′-CAG CTG GGC TGT ACA AAC CTT-3′; reverse: 5′-CAG GTC AAC ATC GGC AAT CA-3′), chemokine (C-C motif) ligand 2 (CCL2) (forward: 5′-GCC AGA CGG GAG GAA GGC CA-3′; reverse: 5′-TGG ATG CTC CAG CCG GCA AC-3′), CCL19 (forward: 5′-GTC GGA GCC TCG GCC TCT CA-3′; reverse: 5′-TGG ATG CTC CAG CCG GCA AC-3′), fructokinase (forward: 5′-GGG AGC AGC CTC ATG GAA GA-3′; reverse: 5′-AGA GCC CAT GAA GGC ACA GC-3′), plasminogen activator inhibitor-1 (PAI-1) (forward: 5′-TCC AAG GGG CAA CGG ATA GA-3′; reverse: 5′-GAC GAA GAG CCA GGC ACA CA-3′), and 18S (forward: 5′-GTA ACC CGT TGA ACC CCA TT-3′; reverse: 5′-CCA TCC AAT CGG TAG TAG CG-3′) were designed using the Primer 3 software (Whitehead Institute for Biomedical Research). For preparation of the PCR mix, Sybr®Green Universal PCR Master Mix (Applied Biosystems) was used. Amplification reactions were carried out in an iCycler (Bio-Rad Laboratories) with an initial hold step (95°C for 3 min) and 50 cycles of a three-step PCR (95°C for 15 s, 60°C for 15 s, and 72°C for 30 s). To monitor amplification of the target gene, the fluorescence intensity of each sample was measured at each temperature change. The amount of target gene, which was normalized to an endogenous reference (18S), was calculated by the comparative C_T method and relative to a calibrator ($2^{-\Delta\Delta Ct}$). The purity of PCR products was verified by melting curves and gel electrophoresis.

Western blot

To prepare cytosolic protein lysates liver tissue was homogenized in a lysis buffer (1 *M* HEPES, 1 *M* $MgCl_2$, 2 *M* KCl, and 1 *M* DTT) containing a protease and phosphatase inhibitors mix (Sigma). Proteins were separated in a 10% sodium dodecyl sulphate–polyacrylamide gel and transferred onto Hybond™-P polyvinylidene difluoride membranes (Amersham Biosciences). Blots were then probed with antibodies against phospho-IκB, total IκB, iNOS, and β-actin (IκB, total IκB, and β-actin [Cell Signaling Technology]; iNOS [Santa Cruz Biotechnology]). Bands were detected using Super Signal Western Dura kit (Thermo Scientific). To ascertain equal loading, all blots were stained with Ponceau red. Protein bands were densitometrically analyzed using the Flurochem Software (Alpha Innotech).

Immunohistochemical staining for MyD88, 4-HNE, 3-NT adducts, and NFκB protein

To determine MyD88, 4-HNE-, 3-NT-protein adducts, and NFκB p65 protein paraffin-embedded liver sections (5 μm) were deparaffinated and rehydrated in ethanol solutions with decreasing concentrations. Liver tissue was stained for MyD88 by blocking slides with 8% BSA in PBS containing 0.1% Tween for 45 min, washing with 2% BSA in PBS containing 0.1% Tween, and an overnight incubation with a polyclonal primary antibody solution (Santa Cruz Biotechnology) in a humidified chamber at 4°C. Liver sections were washed and MyD88 was detected by incubating slides with a peroxidase-linked secondary antibody and diaminobenzidine (Peroxidase Envision Kit; DAKO). 4-HNE adduct staining was performed as previously described (9) using a polyclonal primary antibody (AG Scientific). For determination of 3-NT adducts as well as NFκB p65 protein stainings were performed as described previously (7) using polyclonal primary antibodies (3-NT [Cell Signaling Technology]; NFκB [Santa Cruz Biotechnology]). Finally, 3-NT adducts and NFκB protein were detected by using a commercially available kit (Peroxidase Envision Kit; DAKO). The extent of labeling in liver lobules was defined as percent of the field area within the default color range determined by the software using an image acquisition and analysis system incorporated in the microscope. Data from eight fields (630× with oil immersion for MyD88 and NFκB p65, 200× for 4-HNE and 3-NT) of each tissue section were used to determine means. A negative control of each staining was provided by processing staining procedures like the usual staining but incubating a slide with antibody diluent instead of polyclonal primary antibodies. All sections used for staining ($n = 4$–6 per group) were prepared in parallel and sections for densitometric analyses were stained at the same time. Furthermore, analyses were performed simultaneously.

Endotoxin assay

Plasma samples were heated at 70°C for 20 min to assess endotoxin levels. Using a commercially available limulus amebocyte lysate assay (Charles River) with a concentration range of 0.015–1.2 EU/ml, concentration of endotoxin in plasma of mice was determined.

Statistical analyses

All results are reported as means ± standard error of the mean ($n = 4$–6 per group). One-way ANOVA with Turkey's *post hoc* test was used for the determination of statistical significance among treatment groups. Significance between two groups was determined using the Mann–Whitney test. A p-value <0.05 was selected as the level of significance before the study.

Results

Effect of chronic consumption of fructose-sweetened drinking water on the onset of liver steatosis and insulin resistance

Representative pictures of hematoxylin and eosin as well as oil red O staining of livers are shown in Figure 1A and hepatic triglyceride levels of animals are summarized in Figure 1B. No pathological changes were found in water-fed wild-type or iNOS$^{-/-}$ mice. Triglyceride concentrations in livers of water-fed wild-type and iNOS$^{-/-}$ mice were minimal and did not differ. Chronic intake of 30% fructose solution resulted in a significant ~5-fold increase in hepatic triglyceride accumulation in wild-type mice compared to water-fed groups, an effect also found in histological slides and by oil red O staining. Further, plasma ALT levels of wild-type mice fed fructose were ~5.8-fold higher than those of water-fed controls (Table 1). Despite a similar average fructose intake per gram body weight, triglyceride levels in fructose-fed iNOS$^{-/-}$ mice were only ~2-fold higher than those of water-fed iNOS$^{-/-}$ and wild-type controls (not significant). In line with these findings, neither ALT levels in plasma nor absolute liver weight or liver-to-body-weight ratio of wild-type mice and iNOS$^{-/-}$ mice fed water or fructose differed (Table 1); however, body weight gain did not differ between the two fructose-fed groups (Table 1). Further, markers of hepatic inflammation (*e.g.*, neutrophil infiltration and mRNA expression of chemokine [C-C motif] ligand-2 and −19) were significantly higher in livers of fructose-fed wild-type mice than in water controls. Again, a similar effect of fructose feeding was not detected in livers of iNOS$^{-/-}$ mice.

To determine if the loss of iNOS protected mice from fructose-induced insulin resistance, plasma RBP4 and TNFα levels were determined (Table 1). Indeed, in line with earlier reports of our own group and those of other groups (9, 37), chronic intake of fructose solution resulted in a significant increase of plasma RBP4 and TNFα levels in wild-type mice fed with fructose solution in comparison to water-fed con-

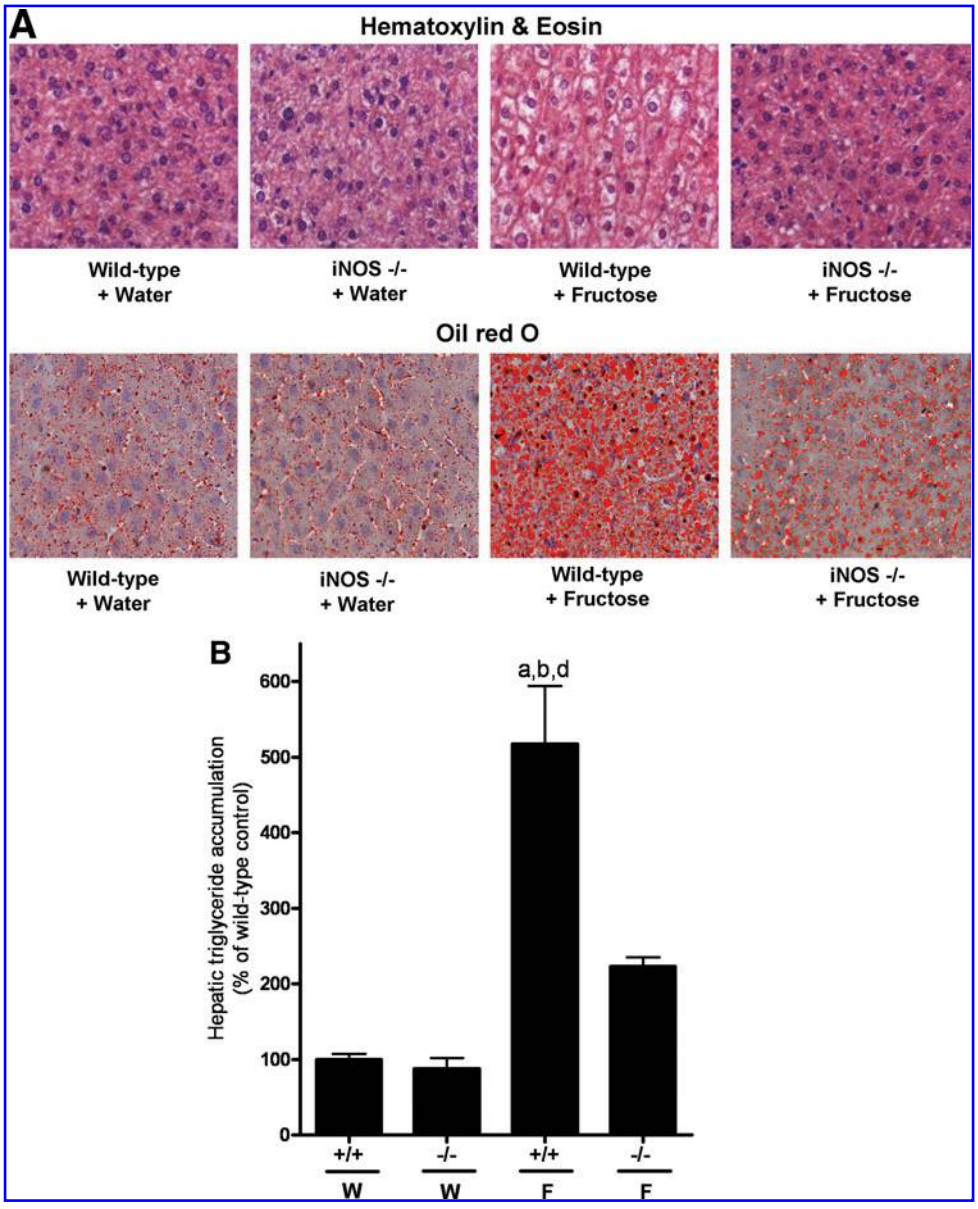

FIG. 1. Effect of chronic consumption of 30% fructose solution on lipid accumulation in the liver. (A) Representative photomicrographs of the hematoxylin and eosin as well as oil red O staining (400×) of liver sections and **(B)** quantification of the hepatic triglyceride accumulation. Data are shown as means ± SEM ($n = 4$–6 per group) and are normalized to percent of wild-type control. W, water; F, 30% fructose solution. $^{a}p < 0.05$ compared with wild-type mice fed water; $^{b}p < 0.05$ compared with iNOS$^{-/-}$ mice fed water; $^{d}p < 0.05$ compared with iNOS$^{-/-}$ mice fed 30% fructose solution. iNOS, inducible nitric oxide synthase; iNOS, iNOS knockout; SEM, standard error of the mean. (To see this illustration in color the reader is referred to the web version of this article at www.liebertonline.com/ars).

Table 1. Fructose Intake, Body Weight, and Indices of Liver Steatosis, Tumor Necrosis Factor-α, and Retinol Binding Protein 4 Plasma Levels as well as Markers of Inflammation in Mice

	Water		*Fructose*	
	Control	*iNOS$^{-/-}$*	*Control*	*iNOS$^{-/-}$*
Weight gain (in g)	3.1 ± 0.1	4.6 ± 0.5	5.2 ± 0.7	5.2 ± 0.5
Liver weight (in g)	1.0 ± 0.0	1.2 ± 0.0	1.5 ± 0.1[a–c]	1.2 ± 0.1
Liver-to-body weight ratio (in%)	4.8 ± 0.1	5.0 ± 0.1	6.0 ± 0.1[a–c]	5.0 ± 0.1
Alanine-aminotransferase (in U/L)[d]	2.8 ± 0.9	1.9 ± 0.3	16.2 ± 4.2[a–c]	5.2 ± 1.0
Fructose intake (in ml/g body weight/day)			2.1 ± 1.3	2.1 ± 1.0
Retinol binding protein 4 (in μg/ml)	19.9 ± 4.6	23.3 ± 3.2	44.9 ± 3.5[a–c]	26.7 ± 6.0
tumor necrosis factor-α (in pg/ml)	7.4 ± 2.7	11.7 ± 1.8	22.1 ± 2.7[a–c]	9.4 ± 2.0
Neutrophil count	0.2 + 0.0	0.1 ± 0.1	1.1 + 0.01[a–c]	0.1 ± 0.0
Chemokine (C-C motif) ligand 2 (CCL2) (% of wild-type control)	100.0 + 24.1	64.1 + 17.0	602.5 + 157.1[a–c]	169.1 + 24.1
CCL19 (% of wild-type control)	100.0 + 23.3	80.9 + 18.3	356.3 + 95.49[a,b]	200.6 + 33.2

Feeding of 30% fructose solution is described in Materials and Methods. Data are means ± standard error of the mean ($n = 4$–5 per group).
[a] $p < 0.05$ compared with iNOS wild-type mice fed water.
[b] $p < 0.05$ compared with iNOS$^{-/-}$ mice fed water.
[c] $p < 0.05$ compared with iNOS$^{-/-}$ mice fed 30% fructose solution.
[d] Normal range: <35 U/L as reported by Tiegs *et al.* (39) before.
iNOS, inducible nitric oxide synthase; iNOS$^{-/-}$, iNOS knockout.

trols. A similar effect of the fructose feeding was not found in iNOS$^{-/-}$ mice.

Hepatic lipid peroxidation, concentration of glutathione, and iNOS protein after chronic consumption of fructose-sweetened drinking water

Concentration of 4-HNE adducts in livers of water-fed animals was minimal and did not differ between substrains (Fig. 2A, B). In livers of wild-type mice chronically exposed to fructose, levels of 4-HNE adducts were significantly higher by ~2.3-fold in comparison to both water-fed wild-type and iNOS$^{-/-}$ mice. In contrast, in iNOS$^{-/-}$ mice fed 30% fructose solution, levels of 4-HNE adducts were reduced almost to the level of controls. In line with these findings, concentration of 3-NT was also found to be significantly higher in livers of fructose-fed wild-type mice (~1.9-fold) than in all other groups (Fig. 2A, C).

GSH and GSSG in whole-liver homogenate did not differ between groups (Fig. 3A, B); however, concentrations varied considerably between animals. In line with our earlier findings, mRNA levels of iNOS were markedly higher in livers of fructose-fed mice than in water-fed controls (Fig. 3C). As to be expected, iNOS protein was not detected in liver samples obtained from iNOS$^{-/-}$ mice regardless of additional treatments (Fig. 3D).

Activation of IκB and NFκB, as well as TNFα mRNA expression in livers of mice after chronic consumption of fructose solution

As it has been suggested by the results of our own group and those of other groups that the development of fructose-induced NAFLD is associated with an increased activation of the redox-sensitive NFκB and an induction of the mRNA expression of TNFα in the liver (9, 30), phosphorylation of IκB, NFκB, and TNFα mRNA expression was determined. Phosphorylation of IκB was significantly higher (~2.4-fold) in wild-type mice fed fructose solution compared to both water-fed groups (Fig. 4A). In contrast, concentration of phospho-IκB in livers of iNOS$^{-/-}$ mice did not differ from that of water controls. In line with these findings, NFκB p65 activity was markedly higher in livers of fructose-fed wild-type mice in comparison to all other groups (Fig. 4B). Further, in livers of fructose-fed wild-type mice NFκB staining was more prominent in Kupffer cells than in all other feeding groups regardless of substrain and treatment. Representative pictures of staining are shown in Figure 4C. In line with these findings, mRNA expression of TNFα mRNA was only found to be induced in livers of wild-type mice fed fructose (+~5-fold in comparison to water controls, $p < 0.05$), whereas in livers of iNOS$^{-/-}$ expression of TNFα, mRNA was at the level of controls (Fig. 4D).

Effect of chronic consumption of fructose solution on portal endotoxin concentration and hepatic MyD88 levels

As it has been suggested by the results of animals studies of our own group that the development of fructose-induced NAFLD and the increased formation of ROS as well as induction of iNOS in the liver is associated with an increased intestinal translocation of bacterial endotoxin and induction of the TLR-4 adaptor protein MyD88 in the liver (9, 17, 21, 37), levels of endotoxin in portal plasma and mRNA

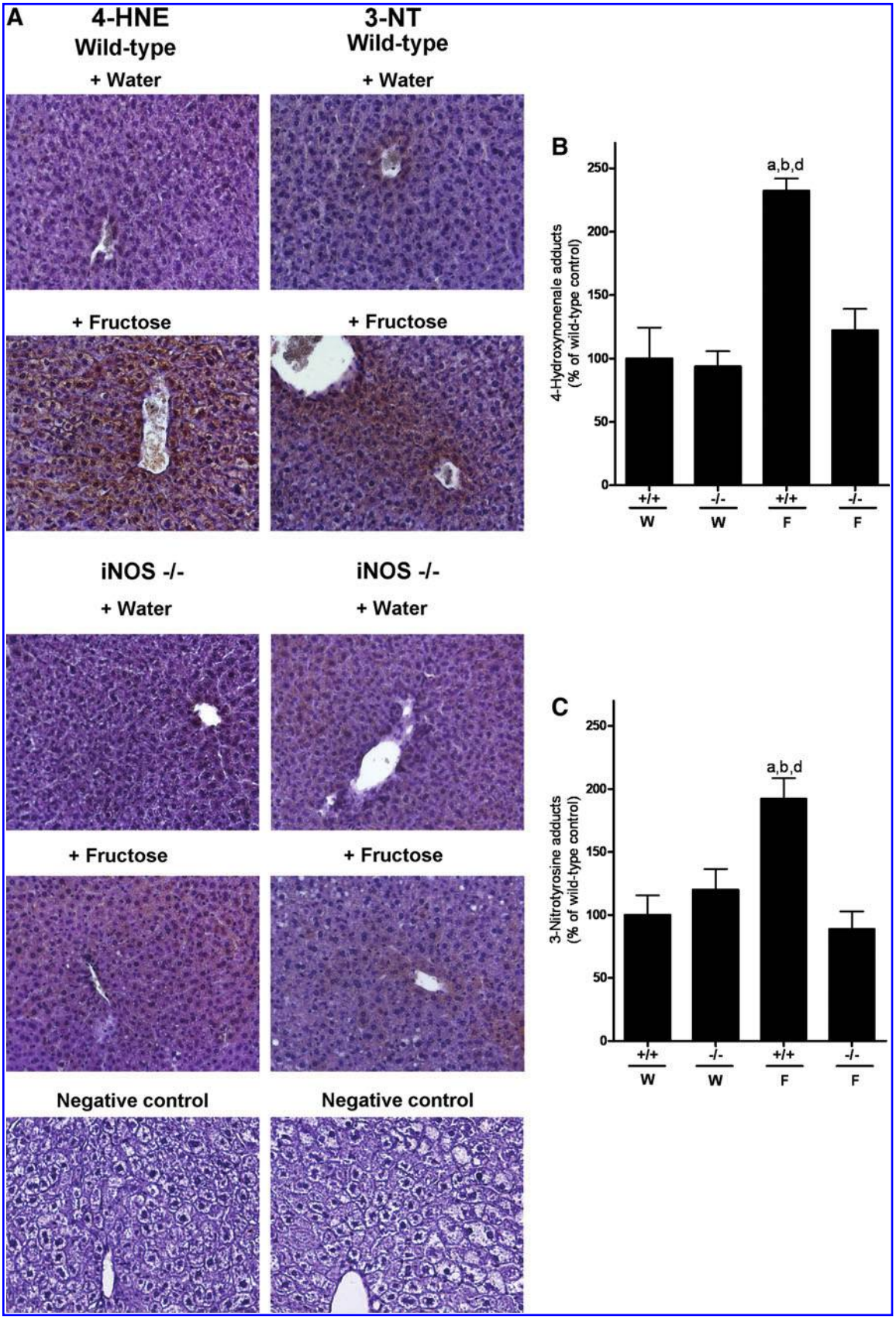

FIG. 2. Effect of chronic consumption of 30% fructose solution on hepatic lipid peroxidation. Representative photomicrographs of immunostaining of **(A)** 4-hydroxynonenal adduct and of 3-nitrotyrosine adduct staining (both 200×) in liver sections. Densitometric analysis of **(B)** 4-hydroxynonenal adduct staining and **(C)** of 3-nitrotyrosine adduct staining. Data are shown as means ± SEM ($n = 4$–6 per group) and are normalized to percent of wild-type control. W, water; F, 30% fructose solution. $^{a}p < 0.05$ compared with wild-type mice fed water; $^{b}p < 0.05$ compared with iNOS$^{-/-}$ mice fed water; $^{d}p < 0.05$ compared with iNOS$^{-/-}$ mice fed 30% fructose solution. (To see this illustration in color the reader is referred to the web version of this article at www.liebertonline.com/ars).

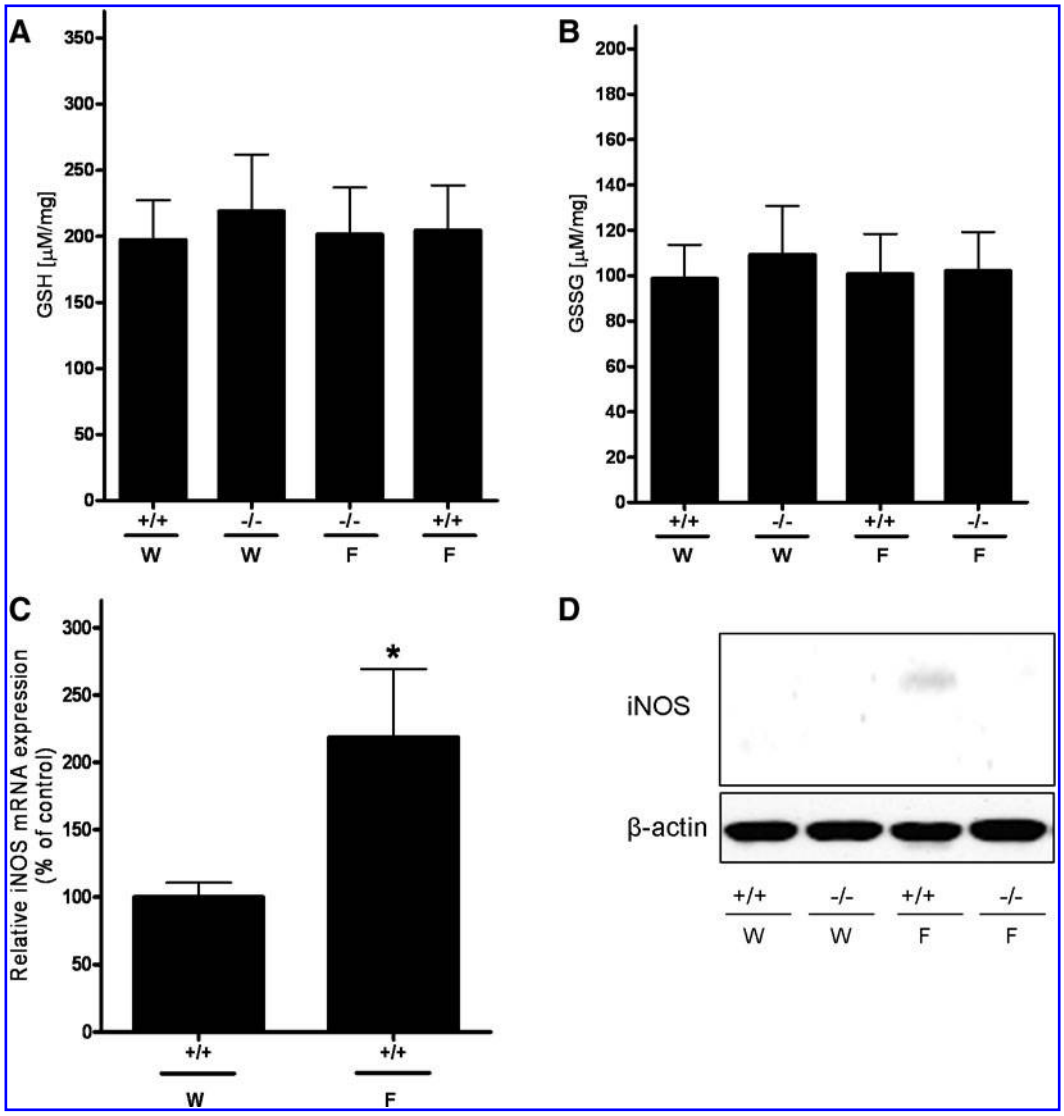

FIG. 3. Effect of chronic consumption of 30% fructose solution on hepatic concentration of reduced and oxidized glutathione as well as expression and protein levels of iNOS. Hepatic concentration of **(A)** reduced and **(B)** oxidized glutathione. **(C)** Expression levels of iNOS in wild-type mice normalized to percent of wild-type control as well as **(D)** representative Western blots of iNOS and β-actin protein. Data are shown as means $\pm$ SEM ($n = 4$–6 per group) and are normalized to percent of wild-type control. W, water; F, 30% fructose solution. *$p < 0.05$ compared with wild-type mice fed water. GSH, reduced glutathione; GSSG, oxidized glutathione.

expression as well as protein levels of MyD88 in the liver were determined (Fig. 5). Endotoxin levels in portal plasma of wild-type and iNOS$^{-/-}$ mice fed with plain water were minimal and did not differ between groups (Fig. 5A). In contrast, plasma endotoxin levels in portal plasma of both wild-type and iNOS$^{-/-}$ mice fed chronically with 30% fructose solution were significantly increased by $\sim$330% and 460%, respectively, in comparison to water-fed controls. In line with these findings, hepatic protein levels of MyD88 were markedly higher in fructose-fed mice irrespective of substrain in comparison to water controls ($\sim$5-fold) (Fig. 5B, C). Similar results were also found when determining MyD88 mRNA expression levels; however, as expression levels varied considerably, only a trend was found ($p = 0.08$) (Fig. 5D).

Effect of endotoxin on iNOS mRNA expression and nitrite formation in RAW 264.7 macrophages

To further determine if endotoxin is involved in the induction of iNOS expression and formation of ROS in Kupffer cells, murine RAW 264.7 macrophages, a cell line used repeatedly by us and others before as a model of hepatic Kupffer cells (21, 29), were challenged with endotoxin for 18 h. Stimulation of RAW 264.7 cells with endotoxin (LPS) resulted in a significant $\sim$30-fold induction of nitrite concentration. This effect of endotoxin was significantly attenuated by $\sim$60% when cells were treated concomitantly with the TLR-4 inhibitor OxPAPC while being exposed to endotoxin (Fig. 6A). Similar results were also found when determining iNOS expression levels in these cells (Fig. 6B)

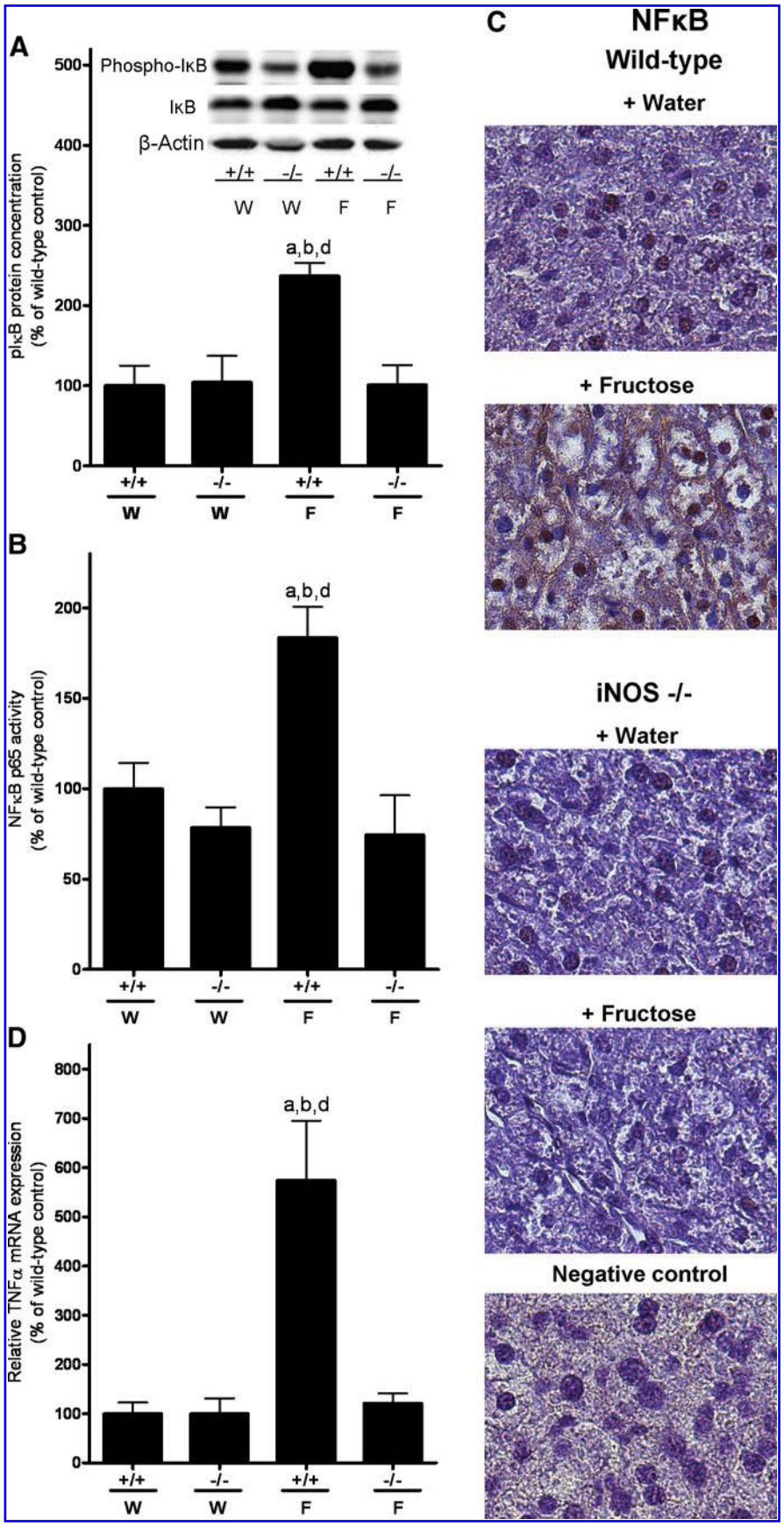

FIG. 4. Effect of chronic consumption of 30% fructose solution on hepatic phosphorylation status of IκB and TNFα mRNA expression level in liver. (A) Phosphorylation of IκB was determined by Western blot and normalized to unphosphorylated IκB in the liver; additionally, β-actin blots are shown as loading control. **(B)** Hepatic activity of NFκB p65 and **(C)** representative photomicrographs of NFκB staining of liver sections. **(D)** TNFα mRNA expression was determined by real-time RT-polymerase chain reaction and normalized to 18S expression in the liver. Data are expressed as means ± SEM ($n = 4$–6 per group) and are normalized to percent of wild-type control. W, water; F, 30% fructose solution. [a]$p < 0.05$ compared with wild-type mice fed water; [b]p 0.05 compared with iNOS$^{-/-}$ mice fed water; [d]$p < 0.05$ compared with iNOS$^{-/-}$ mice fed 30% fructose solution. TNFα, tumor necrosis factor-α. (To see this illustration in color the reader is referred to the web version of this article at www.liebertonline.com/ars).

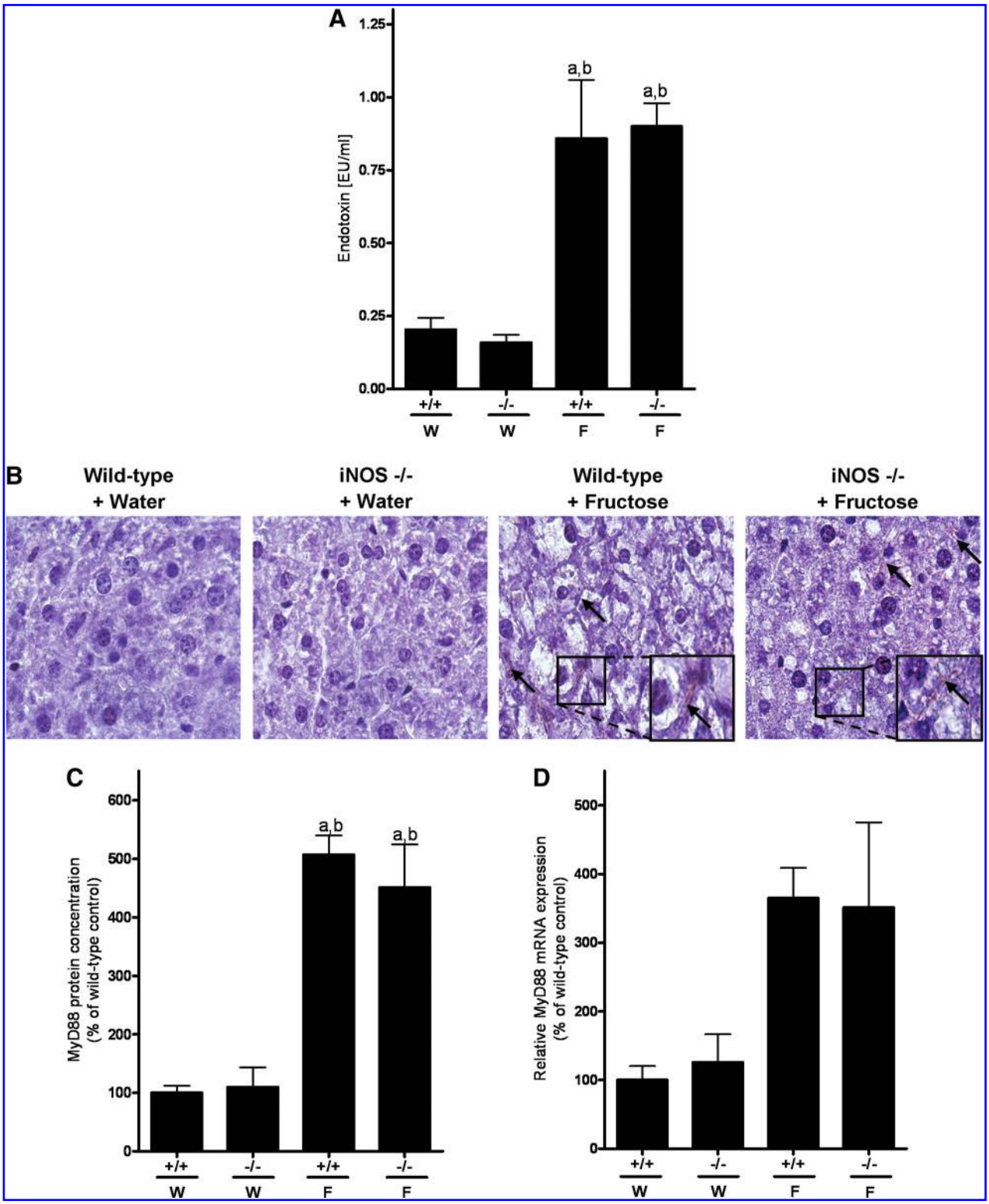

FIG. 5. Effect of chronic consumption of 30% fructose solution on hepatic MyD88 protein concentration and portal endotoxin level. (A) Endotoxin levels in portal plasma. **(B)** Representative photomicrographs (630× with oil immersion; *black arrows* indicate MyD88 protein, stained in brown color) and **(C)** densitometric analysis of immunohistochemical staining for MyD88 protein in liver as well as **(D)** mRNA expression of hepatic MyD88. MyD88 expression levels were normalized to 18S expression. Data are expressed as means ± SEM ($n = 4$–6 per group) and are normalized to percent of wild-type control. W, water; F, 30% fructose solution. $^{a}p < 0.05$ compared with wild-type mice fed water; $^{b}p < 0.05$ compared with iNOS$^{-/-}$ mice fed water. MyD88, myeloid differentiation factor 88. (To see this illustration in color the reader is referred to the web version of this article at www.liebertonline.com/ars).

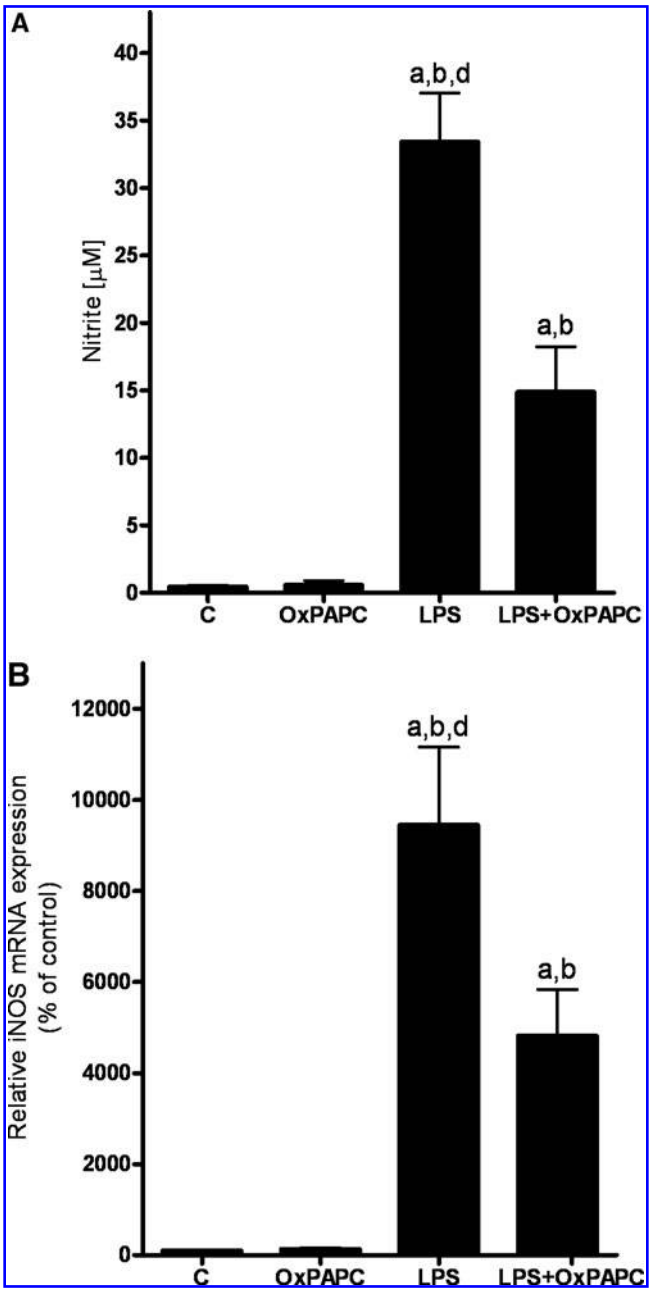

FIG. 6. Effect of LPS on iNOS and nitrite formation in RAW 264.7 cells. (A) iNOS expression and **(B)** nitrite levels in RAW 264.7 cells. Cells were challenged with 50 ng of LPS in the presence of the TLR-4 inhibitor OxPAPC (120 μg/ml) for 18 h. Expression levels were normalized to 18S expression. Data are expressed as means ± SEM ($n = 3$ per group) and are normalized to percent of untreated control. C, untreated cells; OxPAPC, TLR-4 inhibitor OxPAPC; LPS, lipopolysaccharides; LPS + OxPAPC, lipopolysaccharides + TLR-4 inhibitor OxPAPC; TLR-4, toll-like receptor 4. [a]$p < 0.05$ compared to untreated cells; [b]$p < 0.05$ compared to cells treated with the TLR-4 inhibitor OxPAPC; [d]$p < 0.05$ compared to cells treated with the TLR-4 inhibitor OxPAPC + LPS.

Effect of fructose on nitrite formation and on expression of fructokinase in AML-12 cells

To further delineate if fructose itself may cause lipid peroxidation, we challenged AML-12 cells, a model of murine hepatocytes, with fructose at concentrations ranging from 0 to 50 m*M* for 24 h in the presence or absence of the iNOS inhibitor L-NAME. Nitrite levels, used as a marker of iNOS activity, were higher in media obtained from AML-12 cells exposed to L-NAME than in those obtained from naïve cells. However, the presence of 25–50 m*M* fructose in the media had no effect on nitrite formation of cells (Fig. 7A).

In addition, we investigated if iNOS had an effect on fructose metabolism by determining expression of fructokinase mRNA in AML-12 cells exposed to fructose (0–50 m*M*) in the presence or absence of the iNOS inhibitor L-NAME (Fig. 7B). Expression of fructokinase was slightly higher in AML-12 cells exposed to 50 m*M* fructose (+ ~50%; n.s.); however, L-NAME had no additional effect on fructokinase mRNA expression.

Effect of fructose and endotoxin, respectively, on iNOS, TNFα, and PAI-1 mRNA expression in a coculture model of murine RAW 264.7 and AML-12 cells

To further investigate the effect of fructose and endotoxin, respectively, on Kupffer cells and hepatocytes and herein particularly on iNOS expression, a coculture model consisting of RAW 264.7 macrophages and AML-12 cells was developed (for further details, see Materials and Methods). In this model, challenge of RAW 264.7 cells with LPS lead to a significant ~3.5-fold induction of iNOS mRNA expression (Fig. 8A). As expected, when RAW 264.7 cells were concomitantly treated with L-NAME, this effect of LPS was not affected. However, TNFα expression, which was significantly induced in RAW 264.7 macrophages challenged with LPS (+ ~3.5-fold), was attenuated in RAW 264.7 cells concomitantly treated with L-NAME (Fig. 8C). In line with these findings, PAI-1 mRNA expression, which has been shown before to be induced in livers of mice with fructose-induced steatosis in a TNFα receptor 1-dependent way (20), was only significantly induced in AML-12 cells grown in the presence of RAW 264.7 macrophages exposed to LPS (Fig. 8G). In contrast, PAI-1 mRNA expression was at the level of naïve cells in AML-12 cells that were exposed to RAW 264.7 cells concomitantly treated with L-NAME while being challenged with LPS. Further, iNOS mRNA expression was also only found to be induced in AML-12 cells that were exposed to RAW 264.7 cells exposed to LPS (Fig. 8E), whereas iNOS mRNA expression was at the level of naïve controls in AML-12 cells exposed to RAW 264.7 cells concomitantly treated with L-NAME while being challenged with LPS. Interestingly, when RAW 264.6 cells were exposed to fructose, we only found a slight induction of iNOS mRNA expression in RAW 264.7 cells (Fig. 8B), whereas all other parameters remained almost at the level of naïve control cells.

Discussion

Increased carbohydrate and in particular fructose intake has been discussed in recent years to be one of the key factors in the development of obesity, metabolic syndrome (*e.g.*, insulin resistance and dyslipidemia), and NAFLD [for over-

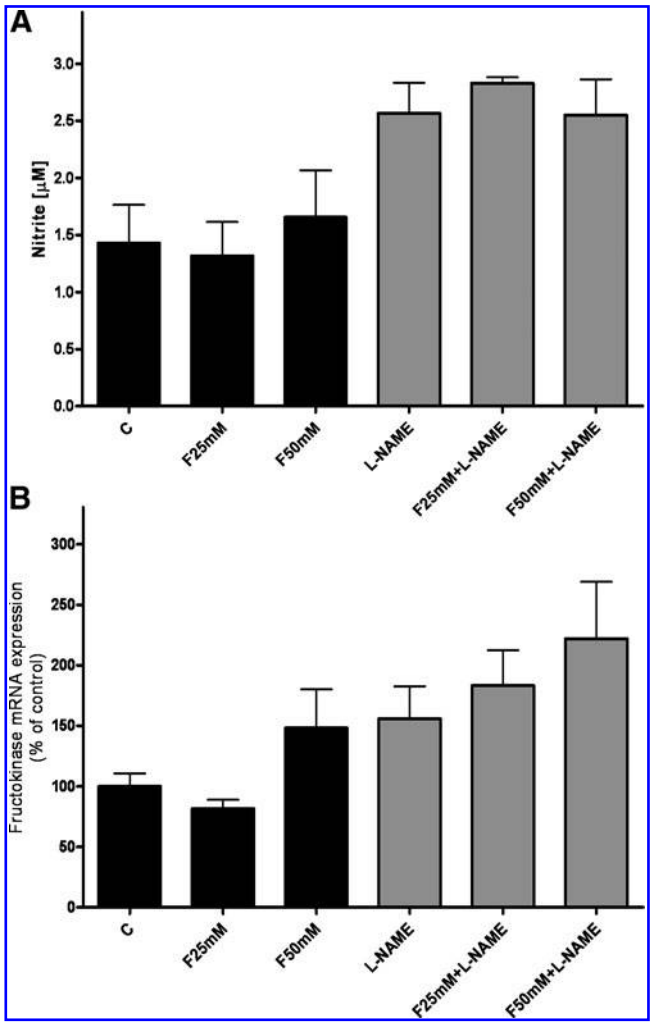

FIG. 7. Effect of fructose on nitrite formation and on fructokinase expression in AML-12 cells. (A) Nitrite concentration and **(B)** fructokinase expression (KHK). Cells were challenged with 0–50 m*M* of fructose in the presence or absence of 10 m*M* L-NAME. Expression levels were normalized to 18S expression. Data are expressed as means ± SEM ($n = 4$ per group) and are normalized to percent of untreated control. C, untreated cells; F25mM, 25 m*M* fructose; F50mM, 50 m*M* fructose; F25mM + L-NAME, 25 m*M* fructose + L-NAME; F50mM + L-NAME, 50 m*M* fructose + L-NAME.

view, also see (36)]. Further, results of animal and human studies suggest that similar to alcoholic liver disease, bacterial overgrowth and increased translocation of bacterial endotoxins across the intestinal barrier may be involved in the pathogenesis of NAFLD (10, 27, 38, 42). Indeed, our own group recently reported that chronic intake of fructose but not glucose causes liver steatosis, which was associated with increased portal endotoxin levels, lipid peroxidation, and an induction of TNFα expression in the liver (9). In these studies we further showed that treatment with nonresorbable antibiotics (9) or the loss of a functional TLR-4 (37) protected the liver from the development of steatosis caused by chronic intake of fructose. However, the exact mechanisms involved in sugar and herein particularly fructose-induced NAFLD are still poorly understood. Here, by feeding mice lacking iNOS chronically with a moderate fructose-enhanced diet (30% fructose in drinking solutions), we further tested the hypothesis that an induction of iNOS associated with chronic intake of fructose is critically involved in the onset of fructose-induced NAFLD. The feeding model employed in the present study, which was developed by our group some years ago on the basis of the study of Jurgens *et al.* (19) to test the effect of different mono- and disaccharides in drinking solutions on the liver (9), has been repeatedly used by us to induce and study the early onset of hepatic steatosis and the metabolic syndrome; however, this model by no means resembles the histology of a steatohepatitis. In line with our earlier findings (37) chronic intake of fructose causes a marked induction of iNOS mRNA expression in livers of wild-type mice. Interestingly, despite similarly elevated portal endotoxin levels and an induction of the TLR-adaptor protein MyD88, which has been shown before by us to be involved in mediating the effects of endotoxin on iNOS mRNA expression in Kupffer cells (21) in livers of $iNOS^{-/-}$ mice fed with fructose solution, hepatic steatosis and markers of inflammation as well as plasma ALT levels were markedly lower than in wild-type controls exposed to fructose. Moreover, the magnitude of protection ($\sim -50\%$) against fructose-induced hepatic steatosis found in livers of $iNOS^{-/-}$ mice fed fructose was similar to that reported earlier by our group for livers of fructose-fed mice treated with nonresorbable antibiotics or mice lacking TLR-4 (9, 37). Further, our results obtained when stimulating RAW 264.7 macrophages with LPS suggest that LPS may lead to an induction of iNOS mRNA expression and nitrite formation but subsequently may also lead to an induction of TNFα and maybe other cytokines (not determined in the present study). Our results further suggest that this may lead to an increased expression of PAI-1 but also iNOS in hepatocytes. A similar effect was not found when RAW 264.7 or AML-12 cells were challenged with fructose, adding further support to the hypothesis that the induction of iNOS found in the present study in livers of wild-type mice exposed to fructose may have resulted from the increased translocation of bacterial endotoxin and subsequent activation of TLR-4-dependent signaling pathways in the liver rather than from direct effects of fructose. Whether the harmful effects of the induction of iNOS result primarily from an induction of this enzyme in Kupffer cells or hepatocytes remains to be determined; however, the results of the present study suggest that an induction of iNOS in Kupffer cells may trigger the induction of iNOS in other cell types in the liver (*e.g.*, hepatocytes). Results of other groups also suggested that an increased formation of ROS is a critical factor in the onset but also in the progression of NAFLD (3, 5, 22). Further, it has been shown in animal studies that by using antioxidants (*e.g.*, silymarin, curcumin, and flavonoid-enriched plant extracts) not only the level of oxidative stress but also liver pathologies can be improved in various models of diet-induced liver damage (*e.g.*, methionine-choline-deficient diet, high-fat diet, and Western-style diet) (14, 15, 23, 26, 32, 40). In the present study, both the significant increase in hepatic 4-HNE and 3-NT adducts found in livers of wild-type mice fed fructose was almost completely blocked $iNOS^{-/-}$ mice fed with fructose. However, levels of GSH and GSSG determined in whole liver homogenate did not differ between strains and feeding groups as levels varied considerable between animals.

Taken together, these data lend further support to the hypothesis that ROS and herein particularly those derived from

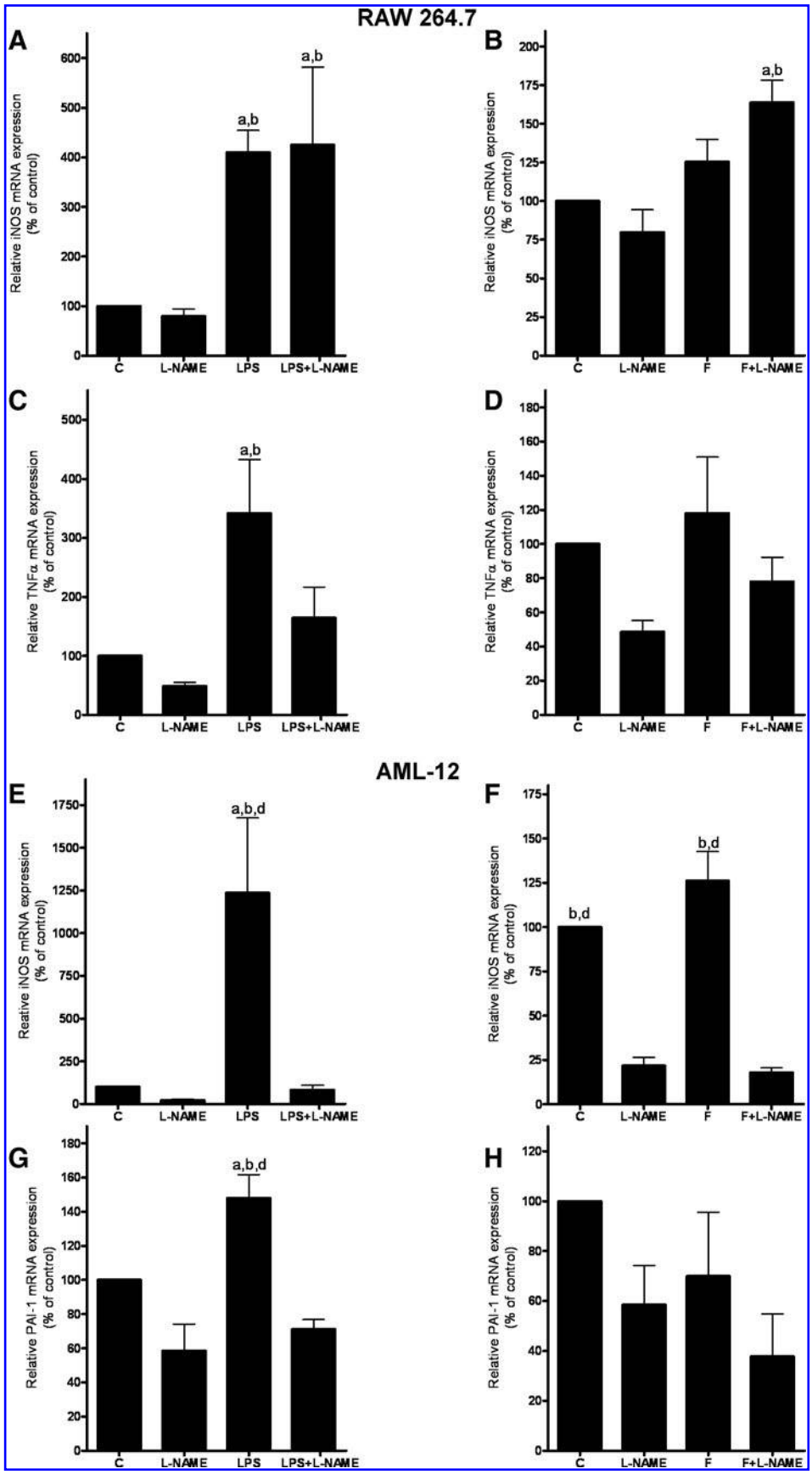

FIG. 8. Effect of fructose and LPS, respectively, on iNOS, TNFα, and plasminogen activator inhibitor-1 mRNA expression in a co-culture model of RAW 265.7 and AML-12 cells. Expression of **(A, B)** iNOS and **(C, D)** TNFα mRNA in RAW 264.7 macrophages. Expression of **(E, F)** iNOS and **(G, H)** plasminogen activator inhibitor-1 mRNA in AML-12 cells. RAW 264.7 cells were treated with LPS (50 mg/ml) or fructose (50 m*M*) in the presence of absence of L-NAME (10 m*M*) before they were cocultured with AML-12 cells. Expression levels were normalized to 18S expression. Data are expressed as means ± SEM ($n = 3$–4 per group) and are normalized to percent of untreated control. C, untreated cells; LPS, lipopolysaccharides; LPS + L-NAME, lipopolysaccharides + L-NAME; F, fructose; F + L-NAME, fructose + L-NAME. [a]$p < 0.05$ compared to untreated cells; [b]$p < 0.05$ compared to cells treated with L-NAME; [d]$p < 0.05$ compared to cells treated with LPS + L-NAME or F + L-NAME, respectively.

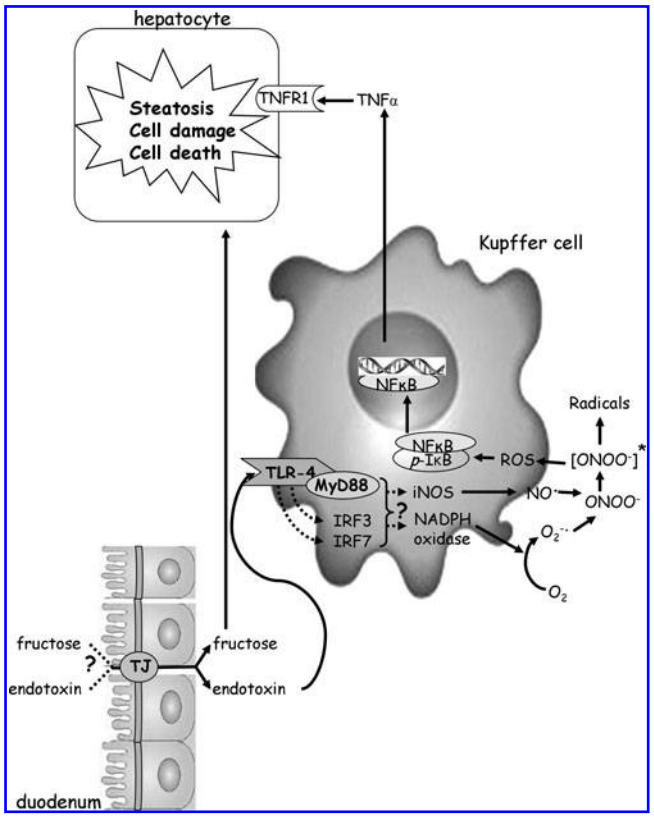

FIG. 9. Working hypothesis of the onset of fructose-induced nonalcoholic fatty liver disease in mice. Chronic fructose consumption may add to hepatic steatosis through its insulin-independent metabolism but also is associated with a loss of tight junction proteins and an increased translocation of intestinal endotoxin into the portal vein. By binding to the endotoxin-receptor TLR4 on the surface of Kupffer cells, Kupffer cells are activated to produce reactive oxygen species *via* iNOS- and/or NADPH-oxidase-dependent pathways. Activation of Kupffer cells induced expression of proinflammatory cytokines like TNFα, which may further add to the onset of hepatic steatosis but also hepatocellular damage and cell death. [$ONOO^-$]*, peroxynitrite in transition state; IRF3/7, interferon regulatory factor 3 or 7; NFκB, nuclear factor κB; $NO^\bullet$, nitric oxide radical; O_2, dioxide; O_2^-, superoxide anion; $ONOO^-$, peroxynitrite; pIκB, phospho-Iκ B; ROS, reactive oxygen species; TJ, tight junctions; TNFR-1, tumor necrosis factor-α receptor-1.

an induction of iNOS in the liver may be a critical factor in the onset of NAFLD and are with this in line with most other reports studying the role of iNOS in the onset and progression of metabolic liver diseases (*e.g.*, alcoholic and nonalcoholic fatty liver disease) (25, 34, 37). However, the results of the present study stand in contrast to those of Rai *et al.* (31) and Chen *et al.* (13), who found that a deletion of iNOS may lead to an impaired liver regeneration and may exacerbate diet-induced liver damage. Differences between these studies and the results of the present study may have resulted from the differences of the cause of liver damage (*e.g.*, fructose enriched diet *vs.* fat and carbohydrate rich diet or partial hepatectomy) or the status of the liver (recovery *vs.* onset and progression of damage). Further, the results of the present study also lend further support to the hypothesis that fructose may not only contribute to the development of NAFLD through mechanisms depending on its insulin-independent metabolism (*e.g.*, through bypassing the main rate-limiting step of glycolysis [for overview, see (36)] but also that an increased translocation of bacterial endotoxin across the intestinal barrier, activation of TLR-4-dependent signalling cascades, and subsequently an induction of the iNOS in the liver may be involved in the beginning of fructose-induced NAFLD (also see Fig. 5). Indeed, in our earlier studies we were able to show that the induction of iNOS and increased levels of 4-HNE adducts found in wild-type mice, which displayed a marked accumulation of lipids after being fed 30% fructose solution for 8 weeks, was markedly attenuated in fructose-fed TLR-4 mutant mice (37).

Results of several studies indicate that TNFα might play a critical role in the pathogenesis of NAFLD. Further, in models of alcoholic liver disease bacterial endotoxins have been shown to induce TNFα in the liver through mechanisms depending on an increased generation of ROS and activation of the redox-sensitive NFκB [for overview, see (6)]. In the present study, both TNFα mRNA expression in the liver and plasma TNFα levels was markedly increased. A similar effect of the chronic feeding of fructose was not found in $iNOS^{-/-}$ mice. Further, the induction of TNFα mRNA expression found in the livers of wild-type mice was associated with an increased phosphorylation of Iκ B and activation of NFκB. Again, a similar effect of chronic fructose intake was not found in livers of $iNOS^{-/-}$ mice. Interestingly, in livers of fructose-fed wild-type mice NFκB staining was more prominent in Kupffer cells than in $iNOS^{-/-}$ mice fed with fructose. A loss of insulin sensitivity has been claimed to be a key factor in the development of NAFLD [for overview, see (24)]. Further, Charbonneau *et al.* (11) recently reported that iNOS may cause hepatic insulin resistance through tyrosine nitration of key insulin signaling proteins. However, iNOS has also been shown before to be an important factor in liver regeneration, in that after partial hepatectomy hepatic steatosis was much more pronounced in mice lacking iNOS than in controls (31). In the present study, not only plasma TNFα levels but also RBP4 plasma concentration, both parameters indicating insulin resistance (16, 33, 43), were markedly higher in wild-type mice chronically fed fructose, whereas these parameters were at the levels of controls in $iNOS^{-/-}$ mice. Further, using a cell culture model of murine hepatocytes we were able to show that iNOS seems not to alter fructose metabolism directly. Taken together, these data further add support to the hypothesis that the deletion of iNOS may have protected mice from fructose-induced steatosis and insulin resistance through interfering with the endotoxin/TLR-4-dependent activation of NFκB and subsequently the induction of TNFα rather than through altering fructose metabolism directly (also see Fig. 9).

Taken together, the results of the present study add further weight to the hypothesis that the damaging effects of chronic fructose consumption may not solely be a result of an increased *de novo* lipogenesis. Rather, our results suggest that an increased formation of ROS is a key event in the onset of fructose-induced fatty liver. Our data further suggest that the activation of iNOS, probably resulting from the increased translocation of bacterial endotoxin and the subsequent induction of TLR-4-dependent signalling pathway, may at least

in part be responsible for the increased formation of ROS found in onset of fructose-induced fatty livers. However, whether similar mechanisms are also applicable in the human situation remains to be determined.

Acknowledgments

This work was supported in part by grants from the German Research Foundation and the Federal Ministry of Education and Research (Grants BE 2376/4-1 [to I.B.] and 03105084 [to I.B.]).

Author Disclosure Statement

No competing financial interests exist.

References

1. Abdelmalek MF, Suzuki A, Guy C, Unalp-Arida A, Colvin R, Johnson RJ, and Diehl AM. Increased fructose consumption is associated with fibrosis severity in patients with nonalcoholic fatty liver disease. *Hepatology* 51: 1961–1971, 2010.
2. Ackerman Z, Oron-Herman M, Grozovski M, Rosenthal T, Pappo O, Link G, and Sela BA. Fructose-induced fatty liver disease: hepatic effects of blood pressure and plasma triglyceride reduction. *Hypertension* 45: 1012–1018, 2005.
3. Ackerman Z, Oron-Herman M, Rosenthal T, Pappo O, Link G, Sela BA, and Grozovski M. Effects of amlodipine, captopril, and bezafibrate on oxidative milieu in rats with fatty liver. *Dig Dis Sci* 53: 777–784, 2008.
4. Adams LA, Lymp JF, St SJ, Sanderson SO, Lindor KD, Feldstein A, and Angulo P. The natural history of nonalcoholic fatty liver disease: a population-based cohort study. *Gastroenterology* 129: 113–121, 2005.
5. Armutcu F, Coskun O, Gurel A, Kanter M, Can M, Ucar F, and Unalacak M. Thymosin alpha 1 attenuates lipid peroxidation and improves fructose-induced steatohepatitis in rats. *Clin Biochem* 38: 540–547, 2005.
6. Arteel GE. Oxidants and antioxidants in alcohol-induced liver disease. *Gastroenterology* 124: 778–790, 2003.
7. Arteel GE. Alcohol-induced oxidative stress in the liver: *in vivo* measurements. *Methods Mol Biol* 447: 185–197, 2008.
8. Bedogni G, Miglioli L, Masutti F, Tiribelli C, Marchesini G, and Bellentani S. Prevalence of and risk factors for nonalcoholic fatty liver disease: the Dionysos nutrition and liver study. *Hepatology* 42: 44–52, 2005.
9. Bergheim I, Weber S, Vos M, Kramer S, Volynets V, Kaserouni S, McClain CJ, and Bischoff SC. Antibiotics protect against fructose-induced hepatic lipid accumulation in mice: role of endotoxin. *J Hepatol* 48: 983–992, 2008.
10. Brun P, Castagliuolo I, Di L, V, Buda A, Pinzani M, Palu G, and Martines D. Increased intestinal permeability in obese mice: new evidence in the pathogenesis of nonalcoholic steatohepatitis. *Am J Physiol Gastrointest Liver Physiol* 292: G518–G525, 2007.
11. Charbonneau A and Marette A. Inducible nitric oxide synthase induction underlies lipid-induced hepatic insulin resistance in mice: potential role of tyrosine nitration of insulin signaling proteins. *Diabetes* 59: 861–871, 2010.
12. Chen Y, Hozawa S, Sawamura S, Sato S, Fukuyama N, Tsuji C, Mine T, Okada Y, Tanino R, Ogushi Y, and Nakazawa H. Deficiency of inducible nitric oxide synthase exacerbates hepatic fibrosis in mice fed high-fat diet. *Biochem Biophys Res Commun* 326: 45–51, 2005.
13. Chen Y, Hozawa S, Sawamura S, Sato S, Fukuyama N, Tsuji C, Mine T, Okada Y, Tanino R, Ogushi Y, and Nakazawa H. Deficiency of inducible nitric oxide synthase exacerbates hepatic fibrosis in mice fed high-fat diet. *Biochem Biophys Res Commun* 326: 45–51, 2005.
14. Garcia-Monzon C, Martin-Perez E, Iacono OL, Fernandez-Bermejo M, Majano PL, Apolinario A, Larranaga E, and Moreno-Otero R. Characterization of pathogenic and prognostic factors of nonalcoholic steatohepatitis associated with obesity. *J Hepatol* 33: 716–724, 2000.
15. Garcia-Ruiz C and Fernandez-Checa JC. Mitochondrial glutathione: hepatocellular survival-death switch. *J Gastroenterol Hepatol* 21 Suppl 3: S3–S6, 2006.
16. Graham TE, Yang Q, Bluher M, Hammarstedt A, Ciaraldi TP, Henry RR, Wason CJ, Oberbach A, Jansson PA, Smith U, and Kahn BB. Retinol-binding protein 4 and insulin resistance in lean, obese, and diabetic subjects. *N Engl J Med* 354: 2552–2563, 2006.
17. Haub S, Kanuri G, Volynets V, Brune T, Bischoff SC, and Bergheim I. Serotonin reuptake transporter (SERT) plays a critical role in the onset of fructose-induced hepatic steatosis in mice. *Am J Physiol Gastrointest Liver Physiol* 298: G335–G344, 2010.
18. Hines IN, Harada H, Bharwani S, Pavlick KP, Hoffman JM, and Grisham MB. Enhanced post-ischemic liver injury in iNOS-deficient mice: a cautionary note. *Biochem Biophys Res Commun* 284: 972–976, 2001.
19. Jurgens H, Haass W, Castaneda TR, Schurmann A, Koebnick C, Dombrowski F, Otto B, Nawrocki AR, Scherer PE, Spranger J, Ristow M, Joost HG, Havel PJ, and Tschop MH. Consuming fructose-sweetened beverages increases body adiposity in mice. *Obes Res* 13: 1146–1156, 2005.
20. Kanuri G, Spruss A, Wagnerberger S, Bischoff SC, and Bergheim I. Role of tumor necrosis factor alpha (TNFalpha) in the onset of fructose-induced nonalcoholic fatty liver disease in mice. *J Nutr Biochem* 2010 [Epub ahead of print]; DOI: 10.1016/j.jnutbio.2010.04.007.
21. Kanuri G, Weber S, Volynets V, Spruss A, Bischoff SC, and Bergheim I. Cinnamon extract protects against acute alcohol-induced liver steatosis in mice. *J Nutr* 139: 482–487, 2009.
22. Levi B and Werman MJ. Long-term fructose consumption accelerates glycation and several age-related variables in male rats. *J Nutr* 128: 1442–1449, 1998.
23. Lin MC, Kao SH, Chung PJ, Chan KC, Yang MY, and Wang CJ. Improvement for high fat diet-induced hepatic injuries and oxidative stress by flavonoid-enriched extract from Nelumbo nucifera leaf. *J Agric Food Chem* 57: 5925–5932, 2009.
24. Malaguarnera M, Di RM, Nicoletti F, and Malaguarnera L. Molecular mechanisms involved in NAFLD progression. *J Mol Med* 87: 679–695, 2009.
25. Mantena SK, Vaughn DP, Andringa KK, Eccleston HB, King AL, Abrams GA, Doeller JE, Kraus DW, rley-Usmar VM, and Bailey SM. High fat diet induces dysregulation of hepatic oxygen gradients and mitochondrial function *in vivo*. *Biochem J* 417: 183–193, 2009.
26. McKim SE, Gabele E, Isayama F, Lambert JC, Tucker LM, Wheeler MD, Connor HD, Mason RP, Doll MA, Hein DW, and Arteel GE. Inducible nitric oxide synthase is required in alcohol-induced liver injury: studies with knockout mice. *Gastroenterology* 125: 1834–1844, 2003.
27. Miele L, Valenza V, La TG, Montalto M, Cammarota G, Ricci R, Masciana R, Forgione A, Gabrieli ML, Perotti G, Vecchio FM, Rapaccini G, Gasbarrini G, Day CP, and Grieco A. Increased

intestinal permeability and tight junction alterations in nonalcoholic fatty liver disease. *Hepatology* 49: 1877–1887, 2009.
28. Ouyang X, Cirillo P, Sautin Y, McCall S, Bruchette JL, Diehl AM, Johnson RJ, and Abdelmalek MF. Fructose consumption as a risk factor for non-alcoholic fatty liver disease. *J Hepatol* 48: 993–999, 2008.
29. Park SY, Baik YH, Cho JH, Kim S, Lee KS, and Han JS. Inhibition of lipopolysaccharide-induced nitric oxide synthesis by nicotine through S6K1-p42/44 MAPK pathway and STAT3 (Ser 727) phosphorylation in raw 264.7 cells. *Cytokine* 44: 126–134, 2008.
30. Ragheb R, Medhat AM, Shanab GM, Seoudi DM, and Fantus IG. Links between enhanced fatty acid flux, protein kinase C and NFkappaB activation, and apoB-lipoprotein production in the fructose-fed hamster model of insulin resistance. *Biochem Biophys Res Commun* 370: 134–139, 2008.
31. Rai RM, Lee FY, Rosen A, Yang SQ, Lin HZ, Koteish A, Liew FY, Zaragoza C, Lowenstein C, and Diehl AM. Impaired liver regeneration in inducible nitric oxide synthasedeficient mice. *Proc Natl Acad Sci U S A* 95: 13829–13834, 1998.
32. Ramirez-Tortosa MC, Ramirez-Tortosa CL, Mesa MD, Granados S, Gil A, and Quiles JL. Curcumin ameliorates rabbits's steatohepatitis via respiratory chain, oxidative stress, and TNF-alpha. *Free Radic Biol Med* 47: 924–931, 2009.
33. Sabio G, Das M, Mora A, Zhang Z, Jun JY, Ko HJ, Barrett T, Kim JK, and Davis RJ. A stress signaling pathway in adipose tissue regulates hepatic insulin resistance. *Science* 322: 1539–1543, 2008.
34. Sanyal AJ, Campbell-Sargent C, Mirshahi F, Rizzo WB, Contos MJ, Sterling RK, Luketic VA, Shiffman ML, and Clore JN. Nonalcoholic steatohepatitis: association of insulin resistance and mitochondrial abnormalities. *Gastroenterology* 120: 1183–1192, 2001.
35. Solga S, Alkhuraishe AR, Clark JM, Torbenson M, Greenwald A, Diehl AM, and Magnuson T. Dietary composition and nonalcoholic fatty liver disease. *Dig Dis Sci* 49: 1578–1583, 2004.
36. Spruss A and Bergheim I. Dietary fructose and intestinal barrier: potential risk factor in the pathogenesis of nonalcoholic fatty liver disease. *J Nutr Biochem* 20: 657–662, 2009.
37. Spruss A, Kanuri G, Wagnerberger S, Haub S, Bischoff SC, and Bergheim I. Toll-like receptor 4 is involved in the development of fructose-induced hepatic steatosis in mice. *Hepatology* 50: 1094–1104, 2009.
38. Thuy S, Ladurner R, Volynets V, Wagner S, Strahl S, Konigsrainer A, Maier KP, Bischoff SC, and Bergheim I. Nonalcoholic fatty liver disease in humans is associated with increased plasma endotoxin and plasminogen activator inhibitor 1 concentrations and with fructose intake. *J Nutr* 138: 1452–1455, 2008.
39. Tiegs G, Kusters S, Kunstle G, Hentze H, Kiemer AK, and Wendel A. Ebselen protects mice against T cell-dependent, TNF-mediated apoptotic liver injury. *J Pharmacol Exp Ther* 287: 1098–1104, 1998.
40. Tipoe GL, Liong EC, Leung TM, and Nanji AA. A voluntary oral-feeding rat model for pathological alcoholic liver injury. *Methods Mol Biol* 447: 11–31, 2008.
41. Venkatraman A, Shiva S, Wigley A, Ulasova E, Chhieng D, Bailey SM, and rley-Usmar VM. The role of iNOS in alcohol-dependent hepatotoxicity and mitochondrial dysfunction in mice. *Hepatology* 40: 565–573, 2004.
42. Wigg AJ, Roberts-Thomson IC, Dymock RB, McCarthy PJ, Grose RH, and Cummins AG. The role of small intestinal bacterial overgrowth, intestinal permeability, endotoxaemia, and tumour necrosis factor alpha in the pathogenesis of non-alcoholic steatohepatitis. *Gut* 48: 206–211, 2001.
43. Yang Q, Graham TE, Mody N, Preitner F, Peroni OD, Zabolotny JM, Kotani K, Quadro L, and Kahn BB. Serum retinol binding protein 4 contributes to insulin resistance in obesity and type 2 diabetes. *Nature* 436: 356–362, 2005.
44. Yang SQ, Lin HZ, Mandal AK, Huang J, and Diehl AM. Disrupted signaling and inhibited regeneration in obese mice with fatty livers: implications for nonalcoholic fatty liver disease pathophysiology. *Hepatology* 34: 694–706, 2001.

Address correspondence to:
Dr. Ina Bergheim
Department of Nutritional Medicine
University of Hohenheim (180 a)
Fruwirthstrasse 12
Stuttgart 70599
Germany

E-mail: ina.bergheim@uni-hohenheim.de

Date of first submission to ARS Central, April 21, 2010; date of final revised submission, November 8, 2010; date of acceptance, November 14, 2010.

Abbreviations Used

3-NT = 3-nitrotyrosine
4-HNE = 4-hydroxynonenal
ALT = alanine-aminotransferase
BSA = bovine serum albumin
GSH = reduced glutathione
GSSG = oxidized glutathione
iNOS = inducible nitric oxide synthase
$iNOS^{-/-}$ = iNOS knockout
IRF3/7 = interferon regulatory factor 3 or 7
L-NAME = Nω-nitro-L-arginine-methylesterhydrochloride
LPS = lipopolysaccharide
MyD88 = myeloid differentiation factor 88
NAFLD = nonalcoholic fatty liver disease
NASH = nonalcoholic steatohepatitis
NFκB = nuclear factor κB
$NO^{\cdot}$ = nitric oxide radical
O_2 = dioxide
$O_2^{-\cdot}$ = superoxide anion radical
$ONOO^-$ = peroxynitrite
$[ONOO^-]^*$ = peroxynitrite in transition state
PAI-1 = plasminogen activator inhibitor-1
PCR = polymerase chain reaction
pIκB = phospho-IκB
RBP4 = retinol binding protein 4
ROS = reactive oxygen species
SEM = standard error of the mean
TJ = tight junctions
TLR-4 = toll-like receptor 4
TNFα = tumor necrosis factor-α
TNFR-1 = tumor necrosis factor-α receptor-1

This article has been cited by:

1. Astrid Spruss, Giridhar Kanuri, Carolin Stahl, Stephan C Bischoff, Ina Bergheim. 2012. Metformin protects against the development of fructose-induced steatosis in mice: role of the intestinal barrier function. *Laboratory Investigation* **92**:7, 1020-1032. [CrossRef]
2. Yuan Liu, Xiaofeng Han, Zhaolian Bian, Yanshen Peng, Zhengrui You, Qixia Wang, Xiaoyu Chen, Dekai Qiu, Xiong Ma. 2011. Activation of Liver X Receptors Attenuates Endotoxin-Induced Liver Injury in Mice with Nonalcoholic Fatty Liver Disease. *Digestive Diseases and Sciences* . [CrossRef]